Numerical Simulation of Vibrationally Active Ar-H2 Microwave Plasma

F. Bosi[1], M. Magarotto[2], P. de Carlo[2], M. Manente[2], F. Trezzolani[2], D. Pavarin [2], D. Melazzi [2], P. Alotto [1], R. Bertani[1]

[1]Department of Industrial Engineering, University of Padova, Padova, Italy
[2]CISAS "G.Colombo", University of Padova, Padova, Italy

Abstract

With the term "vibrational non equilibrium plasma" we refer in general to an ionized molecular gas where the condition $Te \neq Tv \neq T$ is realized. The vibrational non equilibrium between the internal degrees of freedom of a molecule has been first studied by Landau and Teller [1] at the beginning of the century, and has been the subject of considerable attention since then. Much of the work has been devoted to the case $Tv < T$, which is realized typically downstream of shockwaves attached to reentry vehicles in the upper atmosphere, or in shock tube experiments [2].
From a chemical point of view the case $Tv > T$ is more interesting, since it results in catalytic promotion of chemical reactions with high energetic barriers; this phenomenon has been studied between 1970 and the 1990, mostly by Russian researchers [3, 4]; in recent years, there has been a renowned interest on the topic, in order to address environmental and energetic issues.
It has been experimentally and numerically shown [5, 6] that microwave plasma sources can provide efficient dissociation of molecular gases; microwave sources have been studied, for instance, for CO_2 splitting, H_2 plasmas for diamond film deposition and deuterium ion production; however, to our knowledge, numerical investigations, accounting for the vibrational dynamic of the plasma, in the case $Tv>T$, have been restricted till now to global kinetic models.
In this work we simulate an Ar-H_2 gas subject to microwave heating in sub-atmospheric conditions, with a reduced kinetic dataset of reactions reported in Figure 1; from a mathematical point of view the problem can be solved coupling the Maxwell equations for the propagation of the electric field, together with the continuity, momentum and energy equations for the fluid in the Euler simplified form.
For this purpose we use COMSOL Multiphysics® with four interfaces coupled together: the Microwave Plasma interface, the Laminar Flow interface, one PDE interface to solve the total energy equation and one PDE interface to solve the vibrational energy equation. The catalytic effect of the supra thermal vibrational population, results in an enhancement of the rate of unimolecular dissociation (by a factor $\Phi(T,Tv)$, which is addressed with the Kuznetsov [7] model (see Figure 2); in this situation the chemistry of the discharge is coupled to three temperatures solved by the model (i.e. Te, Tv, T).
Results of the simulation are compared to thermal equilibrium case ($Tv = T$) to evaluate to which extent the inclusion of a vibrational dynamic affects the calculations. Preliminary results of vibrational to gas temperature ratio, of Ar:H_2 1:0.1 plasma at 1 Torr are shown in

Figure 3.

Reference

[1] E. E. Nikitin and J. Troe, 70 Years of Landau-Teller Theory for Collisional Energy Transfer. Semiclassical Three-Dimensional Generalizations of the Classical Collinear Model, Physical Chemistry Chemical Physics, Vol. 10, p. 1483 (2008)
[2] J. D. Anderson Jr., Modern Compressible Flow with Historical Perspective (1982)
[3] B. F. Gordiets et al., Non-Equilibrium Dissociation Processes and Molecular Lasers, Soviet Journal of Experimental and Theoretical Physics, Vol. 34, p. 299 (1972)
[4] V. D. Rusanov et al., The Physics of a Chemically Active Plasma with Non-Equilibrium Vibrational Excitation of Molecules, Soviet Physics Uspekhi, Vol. 24, p. 447 (1981)
[5] A. Fridman, Plasma Chemistry, Cambridge University Press (2008)
[6] R. Aerts et al., Influence of Vibrational States on CO2 Splitting by Dielectric Barrier Discharges, The Journal of Physical Chemistry C, Vol. 116, p. 23257 (2012)
[7] G. G. Chernyi et al., Physical and Chemical Processes in Gas Dynamics: Cross sections and rate constants, Vol. I, AIAA (2002)
[8] M. A. Lieberman and A. J. Lichtenberg, Principles of Plasma Discharges and Materials Processing, John Wiley & Sons (2005)
[9] L. Pitchford et al., Comparisons of sets of electron-neutral scattering cross sections and calculated swarm parameters in N2 and H2, In APS Meeting Abstracts, Vol. 1, p. 1087 (2012)
[10] lxcat - Plasma Data Exchange Project, http://nl.lxcat.net/home/ , LX-cat.
[11] T. Kimura and H. Kasugai, Properties of Inductively Coupled Rf Ar/H2 Plasmas: Experiment and Global Model, Journal of Applied Physics, Vol. 107, p. 083308 (2010)
[12] I. Mendez et al., Atom and Ion Chemistry in Low Pressure Hydrogen Dc Plasmas, The Journal of Physical Chemistry A, Vol. 110, p. 6060 (2006)
[13] D. Lymberopoulos and D. Economou, Two-Dimensional Self-Consistent Radio Frequency Plasma Simulations Relevant to the Gaseous Electronics Conference Rf Reference Cell, J. Res. Nat. Inst. Stand. Technol, Vol. 100 i4, p. 473 (1996)
[14] NIST- NIST Chemical Kinetics Database, http://kinetics.nist.gov/kinetics/index.jsp.

Figures used in the abstract

Reaction	Rate Constant 2nd order (cm^3/s) 3rd order (cm^6/s)	Reference
Elastic scattering		
$e + Ar \rightarrow e + Ar$	integrated cross section	[8]
$e + H_2 \rightarrow e + H_2$	integrated cross section	[9, 10]
Rotational and vibrational excitation		
$e + H_2 \rightarrow e + H_2(J_{0\text{-}2})$	integrated cross section	[9, 10]
$e + H_2 \rightarrow e + H_2(J_{1\text{-}3})$	integrated cross section	[9, 10]
$e + H_2 \rightarrow e + H_2(v1)$	integrated cross section	[9, 10]
$e + H_2 \rightarrow e + H_2(v2)$	integrated cross section	[9, 10]
$e + H_2 \rightarrow e + H_2(v3)$	integrated cross section	[9, 10]
Electron impact excitation, and dissociation		
$e + Ar \rightarrow e + Ar(4s)$	$5.0 \cdot 10^{-9} T_e^{0.74} \exp(-11.56/T_e)$	[8]
$e + Ar(4s) \rightarrow e + Ar$	$4.3 \cdot 10^{-10} T_e^{0.74}$	[8]
$e + H_2 \rightarrow e + H + H$	$1.2 \cdot 10^{-8} \exp(-10.0/T_e)$	[11]
Electron impact ionization		
$e + Ar \rightarrow e + Ar^+$	$2.34 \cdot 10^{-8} T_e^{0.59} \exp(-17.44/T_e)$	[8]
$e + Ar(4s) \rightarrow e + Ar^+$	$6.8 \cdot 10^{-9} T_e^{0.67} \exp(-4.20/T_e)$	[8]
$e + H_2 \rightarrow e + e + H_2^+$	integrated cross section	[9, 10]
Electron-ion recombination		
$e + H_2^+ \rightarrow H + H$	$8.0 \cdot 10^{-8} \exp(-0.2/T_e)$	[11]
$e + H_3^+ \rightarrow H_2 + H$	$1.55 \cdot 10^{-6}(300.0/T)$	[11]
$e + H_3^+ \rightarrow H + H + H$	$4.2 \cdot 10^{-9} + 1.5 \cdot 10^{-9} T_e - 1.9 \cdot 10^{-10} T_e^2$	[12]
Charge exchange and neutral reactions		
$H_2 + H_2^+ \rightarrow H_3^+ + H$	$2.1 \cdot 10^{-9}$	[11]
$Ar(4s) + Ar(4s) \rightarrow Ar + e + Ar^+$	$6.2 \cdot 10^{-10}$	[13]
$Ar(4s) + Ar \rightarrow Ar + Ar$	$3.0 \cdot 10^{-15}$	[13]
$H_2 + H_2 \rightarrow H_2 + H + H$	$\Phi(T, T_v) \cdot 3.64 \cdot 10^{-8}(298/T) \exp(-51840/T)$	[14]
$H + H + H_2 \rightarrow H_2 + H_2$	$8.85 \cdot 10^{-33}(298/T)^{0.6}$	[14]
$H_2 + H \rightarrow H + H + H$	$\Phi(T, T_v) \cdot 2.54 \cdot 10^{-8}(298/T)^{0.1} \exp(-52562/T)$	[14]
$H + H + H \rightarrow H + H_2$	$8.82 \cdot 10^{-33}$	[14]
$Ar + H_2 \rightarrow Ar + H + H$	$\Phi(T, T_v) \cdot 1.88 \cdot 10^{-8}(298/T)^{1.1} \exp(-52562/T)$	[14]
$H + H + Ar \rightarrow H_2 + Ar$	$5.93 \cdot 10^{-33}(298/T)$	[14]
Surface reactions	Recombination factor	
$Ar^+ \rightarrow Ar$	$\gamma = 1$	
$Ar(4s) \rightarrow Ar$	$\gamma = 1$	
$H_3^+ \rightarrow H_2 + H$	$\gamma = 1$	
$H_2^+ \rightarrow H_2$	$\gamma = 1$	
$2H \rightarrow H_2$	$\gamma = 0.02$	

1. T_e is in eV

Figure 1: Kinetic dataset.

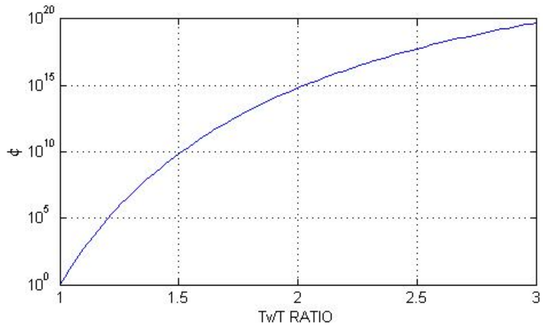

Figure 2: Non equilibrium factor versus Tv/T ration for H2 at T = 500K.

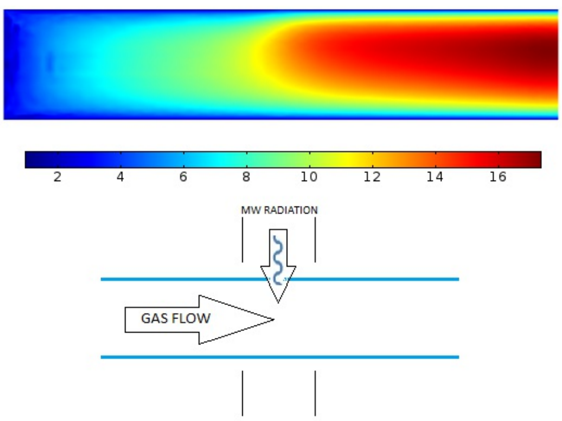

Figure 3: Tv/T ratio of 1 Torr, 1000W microwave plasma (Ar:H2 1:0.1).